MINNESOTA GEOLOGICAL SURVEY
INFORMATION CIRCULAR 47

COMPOSITIONS OF RIFT-RELATED VOLCANIC ROCKS OF THE KEWEENAWAN SUPERGROUP ATOP THE ST. CROIX HORST, SOUTHEASTERN MINNESOTA

UNIVERSITY OF MINNESOTA

Minnesota Geological Survey
D.L. Southwick, *Director*

Information Circular 47

COMPOSITIONS OF RIFT-RELATED VOLCANIC ROCKS OF THE KEWEENAWAN SUPERGROUP ATOP THE ST. CROIX HORST, SOUTHEASTERN MINNESOTA

By

G.B. Morey

UNIVERSITY OF MINNESOTA
St. Paul, 2001

This publication is accessible from the home page of the Minnesota Geological Survey (http://www.geo.umn.edu/mgs) as a PDF file readable with Acrobat Reader 4.0.

Date of release: May, 2001

Recommended citation:

Morey, G.B., 2001, Compositions of rift-related volcanic rocks of the Keweenawan Supergroup atop the St. Croix horst, southeastern Minnesota: Minnesota Geological Survey Information Circular 47, 27 p.

Minnesota Geological Survey
2642 University Avenue West
Saint Paul, Minnesota 55114-1057

Telephone: 612-627-4780
Fax: 612-627-4778
E-mail address: mgs@tc.umn.edu
Web site: http://www.geo.umn.edu/mgs

ISSN 0544-3105

CONTENTS

FIGURES

TABLES

COMPOSITIONS OF RIFT-RELATED VOLCANIC ROCKS OF THE KEWEENAWAN SUPERGROUP ATOP THE ST. CROIX HORST, SOUTHEASTERN MINNESOTA

G.B. Morey

INTRODUCTION

This information circular summarizes stratigraphic and geochemical information obtained in the 1980s and early 1990s from Mesoproterozoic volcanic rocks associated with the Midcontinent rift system. These rift-related rocks comprise the St. Croix horst, a major structural feature now mostly buried by a thin cover of generally flat-lying sedimentary rocks of Paleozoic age. Although the studies described herein were completed 10 to 15 years ago, the results have never been published. This report is intended to correct that omission.

REGIONAL SETTING

The 1,100 million-year-old Midcontinent rift system extends north-northeast from Kansas for about 2,000 km to Lake Superior, and then southeast through Michigan (Fig. 1). The rift is almost completely buried beneath a cover of Paleozoic and younger sedimentary strata; its position has been deduced from gravity and magnetic anomalies (VanSchmus and Hinze, 1985 and references therein). However, significant exposures of rift-related rocks do occur around the margin of Lake Superior. There, surface rocks are a bimodal suite of mostly tholeiitic basalt and some alkaline basalt along with minor silicic rocks (Basaltic Volcanism Study Project, 1981; Brannon, 1984; Paces, 1988; Nicholson, 1992). The alkaline rocks are more abundant in the lower part of the stratigraphic sequence whereas tholeiitic rocks become more abundant up-section.

U-Pb zircon dating of basal volcanic rocks and related sills around the shores of Lake Superior imply that rift-related magmatism began about 1,108.8 + 4/-2 Ma (Davis and Sutcliffe, 1985) during a period of reversed magnetic polarity. The magnetic polarity shifted back to normal between 1,097.6 ± 8.7 Ma and 1,086.5 + 1.3/- 3.0 Ma (Palmer and Davis, 1987). Although volcanism was active in the Lake Superior region for about 22 m.y., most of the activity was restricted to the 3 to 5 m.y. interval shortly after 1,097 m.y. (Davis and Paces, 1990).

Very few drill holes penetrate the rift-related rocks south and west of Lake Superior; however, several sampled volcanic sequences in southern Kansas have chemical characteristics similar to those associated with the rocks exposed around Lake Superior (Cullers and Berendsen, 1993). The basaltic sequence in Kansas is subalkalic to alkalic and follows tholeiitic trends: a number of individual flows of high-alumina basalt are scattered throughout the sequence.

GEOLOGY OF THE ST. CROIX HORST

The generally accepted tectonic model of the Midcontinent rift system in east-central and southeastern Minnesota is that of a central horst—the St. Croix horst—bounded by high-angle faults, partly covered by clastic rocks, and flanked by basins filled with somewhat younger clastic strata (Fig. 2). Both the volcanic and sedimentary rocks are assigned to the Keweenawan Supergroup.

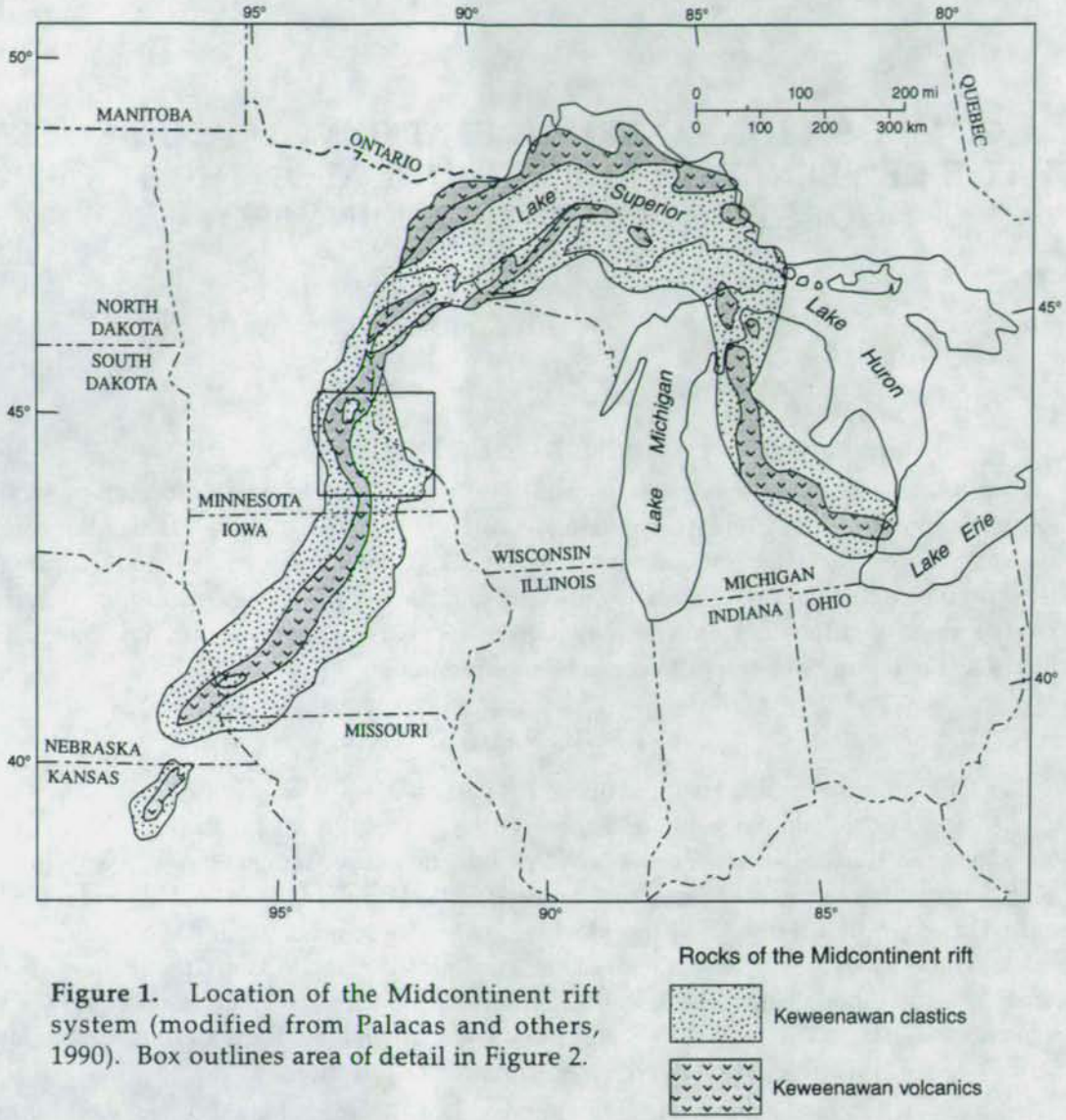

Figure 1. Location of the Midcontinent rift system (modified from Palacas and others, 1990). Box outlines area of detail in Figure 2.

The St. Croix horst is delineated on the northwest by a series of steeply inclined, northeast-trending faults including the Douglas and Pine faults, on the southeast by the Hastings and Cottage Grove faults, and on the southwest by a series of northwest-trending faults including the Belle Plaine fault (Morey, 1977).

In the early 1970s, all of the volcanic rocks that collectively define the St. Croix horst were assigned to the Chengwatana Volcanic Group (Morey and Mudrey, 1972). Lithic sandstone, siltstone, and shale assigned to the Oronto Group occur atop the horst in an east-northeast-plunging basin—the Ashland syncline—located in northwestern Wisconsin and adjoining parts of Minnesota. A second basin atop the southern part of the St. Croix horst is also filled with lithic sandstone, siltstone and shale and is assigned to the Solor Church Formation. This basin, called the Pre-Paleozoic Twin Cities basin, underlies the much younger Twin Cities basin developed in overlying Paleozoic strata (Mossler and Tipping, 2000). Geophysical data indicate that a narrow strip of volcanic rocks on the east side of the pre-Paleozoic basin is in fault contact with rocks of the Solor Church Formation within the basin. This faulted block—the Hudson–Afton horst (Sims and Zietz, 1967)—was uplifted

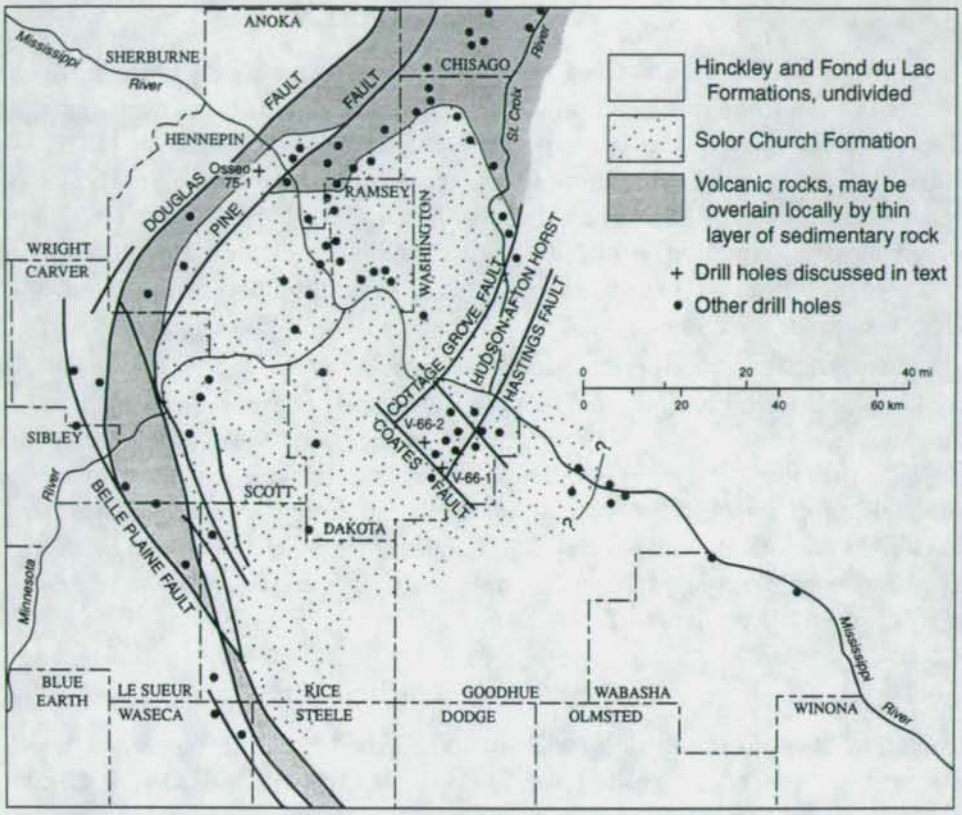

Figure 2. Generalized geologic map of the St. Croix horst in east-central Minnesota and adjoining parts of northwestern Wisconsin. Map based on aeromagnetic data summarized in Cannon and others (2001).

in very Late Cambrian to very Early Ordovician time and is bounded on the west by the Cottage Grove fault, on the east by the Hastings fault, and on the southwest by the Coates fault. The extensive movement which led to the development of the Hudson–Afton horst juxtaposed older extrusive rocks against younger Paleozoic sedimentary rocks. Sims and Zietz (1967) estimated that there has been at least 8,000 to 9,000 feet (2,440 to 2,740 meters) of movement along the Cottage Grove fault.

In the late 1970s, sedimentary rocks assigned to the Solor Church Formation were broadly correlated with those assigned to the Oronto Group to the north. However, recent aeromagnetic data (Cannon and others, 2001) imply that the Chengwatana Volcanic Group (as originally defined by Morey and Mudrey, 1972) is composed of at least five volcanic sequences laid down in a series of structurally and possibly temporally overlapping basins. Several of the basins seem separated by angular unconformities that could be marked by accumulations of clastic sedimentary rock of varying thicknesses. These complex stratigraphic and structural relationships are as yet unresolved, but they raise doubts about existing ideas concerning correlations between the various volcanic and sedimentary entities that comprise the horst.

To better understand these structural and stratigraphic relationships, I report here the compositional characteristics of a series of dominantly felsic volcanic rocks intersected in the Vermillion area on the Hudson–Afton segment, and the compositional characteristics of a thick sequence of mafic volcanic rocks intersected in the Osseo area along the west side of the St. Croix horst.

VERMILLION AREA

In 1966, the Northern Natural Gas Company drilled a series of core holes in Dakota County near the village of Vermillion in search of reservoirs suitable for storing natural gas underground (Fig. 2). Ten holes penetrated beds of shale and lithic sandstone that Morey (1977) assigned to the Solor Church Formation. Two of those holes, approximately one mile apart, also penetrated extrusive igneous rocks classified as undivided volcanic rocks (Morey, 1977). These two volcanic sequences were labeled Vermillion 66-1 (V-66-1) and Vermillion 66-2 (V-66-2). Although drill reports show that 525 feet of volcanic rocks were penetrated at Vermillion 66-1, only 40 feet of core, from 1,055 to 1,095 feet deep, were preserved.

Subsequently, M.E. Cavaleri re-examined the Vermillion 66-1 and Vermillion 66-2 sequences in the early 1980s. He found Vermillion 66-1 to be dominantly composed of basalt and to include one 18-foot-thick felsic unit (Fig. 3). He recognized seven felsite flows and welded tuft units in Vermillion 66-2. Individual flow units range in thickness from one to 70 feet. Cavaleri briefly described the felsic rocks in both holes as "aphyric," or containing sparse feldspar microlites, and typically dark-red to reddish-brown in color. Most of the flows are characterized by strong foliation. He also acquired considerable geochemical data including major, minor, and trace elements (including REE), reproduced here in Tables 1 and 2.

Descriptive Geochemistry

The chemical compositions of the felsic rocks collected from the Vermillion area show that they have been affected by alteration. In terms of $K_2O + Na_2O$ and $K_2O/(K_2O + Na_2O)$ composition, most unaltered rocks lie between two field boundaries that define an igneous spectrum (Hughes, 1973). Figure 4 shows that the felsic rocks from V-66-2 have enhanced alkali abundances relative to the igneous spectrum, and therefore were apparently subjected to metasomatic processes most likely involving the addition of alkalis.

When classified according to SiO_2, K_2O and Na_2O contents (LeBas and others, 1986), samples from Vermillion 66-1 lie within the fields of basaltic trachyandesite or trachydacite (Fig. 5). In contrast, felsic rocks from Vermillion 66-2 are clearly rhyolitic in composition with one exception, a trachybasalt.

Although the sample set is small, most of the rhyolitic rocks in a plot of alkalis versus silica are subalkaline, whereas samples having smaller silica contents tend to plot in the alkali field or along the boundary between the alkaline and subalkaline fields (Fig. 6). Additionally, the analyzed samples tend to follow tholeiitic trends in an AFM diagram (Fig. 7). On a Jensen cation plot, which relies on the concentrations of elements that are generally stable during secondary processes (Jensen, 1976), felsic rocks from the Vermillion area lie on the tholeiitic side along and close to the boundary between tholeiitic and calc-alkalic rocks (Fig. 8).

Major Oxides And Trace Elements

Major-oxide compositions are illustrated in Figure 9 where SiO_2 concentrations are used as a fractionation index. In general, Al_2O_3, MgO, TiO_2, CaO, and P_2O_5 concentrations, as well as the Mg number, decrease as SiO_2 increases. In modern unaltered rhyolite, Na_2O and K_2O concentrations remain generally unequal (Ewart, 1979; LeMaitre, 1984). However, within individual flows in the Vermillion area, K_2O concentrations range widely from unequal (3 to 5 wt. percent) to about 7 to 8 wt. percent and tend to increase with increasing silica content. Most samples contain only minor quantities of Na_2O. Thus, metasomatism in these rocks is almost always in the direction of increasing K_2O contents.

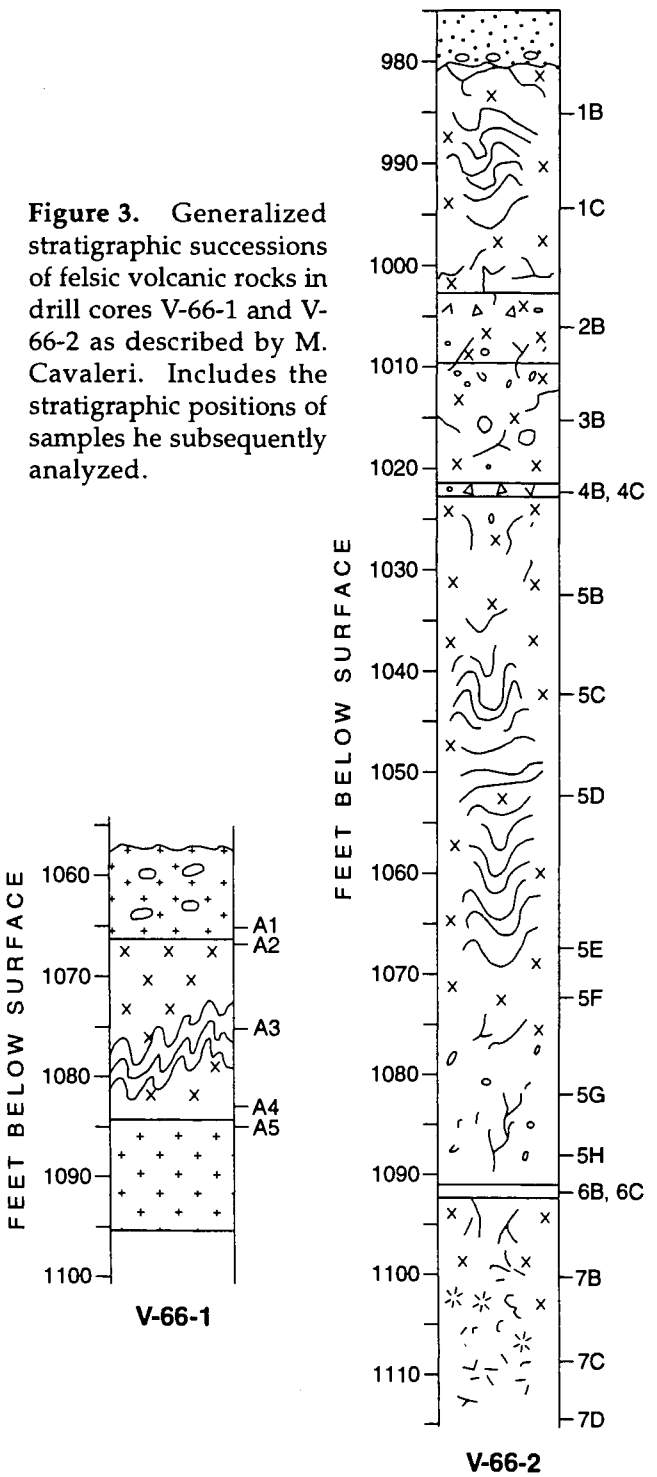

Figure 3. Generalized stratigraphic successions of felsic volcanic rocks in drill cores V-66-1 and V-66-2 as described by M. Cavaleri. Includes the stratigraphic positions of samples he subsequently analyzed.

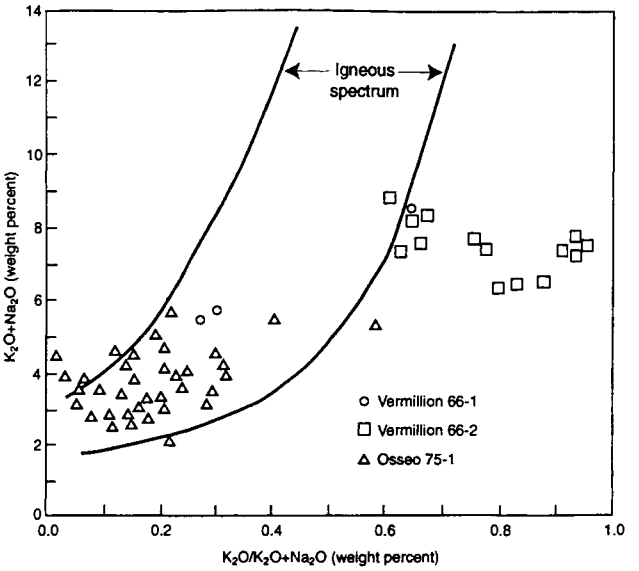

Figure 4. $K_2O + Na_2O$ and $K_2O/(K_2O + Na_2O)$ compositions of volcanic rocks from the Vermillion and Osseo areas. Most unaltered igneous rocks lie between the two field boundaries of the igneous spectrum (after Hughes, 1973). In contrast to the mafic rocks from the Osseo core, the samples from the Vermillion cores show greater K_2O contents than most igneous rocks.

Figure 5. Classification of volcanic rocks from the Vermillion and Osseo areas according to their $K_2O + Na_2O$ and SiO_2 contents (after LeBas and others, 1986).

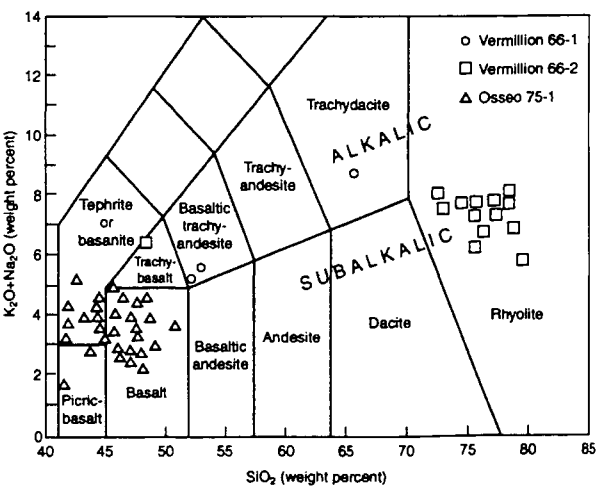

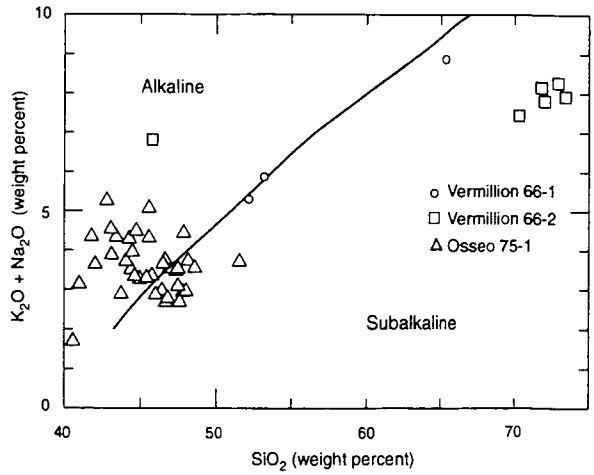

Figure 6. Total alkali versus silica concentrations in the volcanic rocks from the Vermillion and Osseo areas (after Irvine and Baragar, 1971).

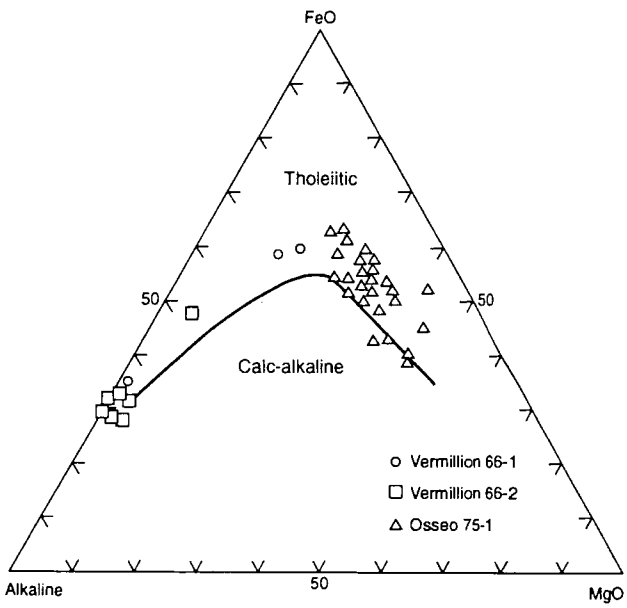

Figure 7. AFM diagram of volcanic rocks from the Vermillion and Osseo areas (after Irvine and Baragar 1971).

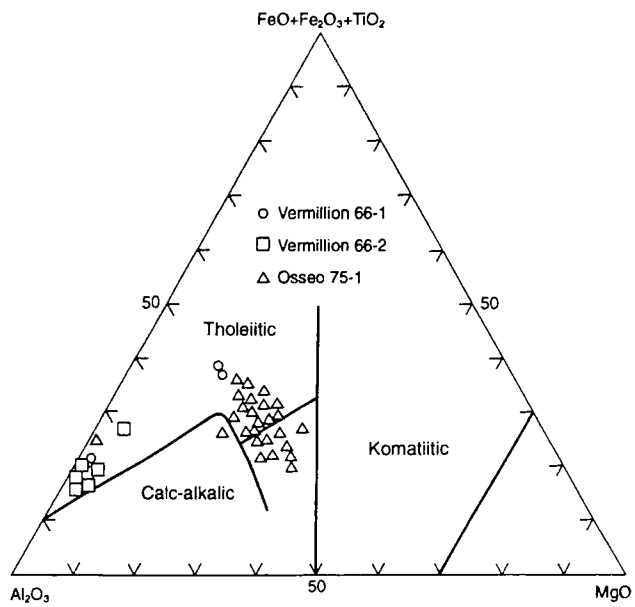

Figure 8. Cation diagram (Jensen, 1976) of volcanic rocks from the Vermillion and Osseo areas. The samples lie within the tholeiitic field and appear to represent two distinct compositional populations.

Comparisons of trace-element abundances in the samples from the two sites are summarized in Figures 10 and 11. Both sets are strongly enriched in lead and depleted in strontium. Rare earth element patterns (Figs. 12 and 13) are typically flat and somewhat enriched in the light rare earth elements relative to the heavy rare earth elements. Interestingly, the samples from Vermillion 66-1 lack the pronounced negative Europium anomalies so prevalent in the rhyolitic samples from Vermillion 66-2.

OSSEO AREA

In 1975, the Northern Natural Gas Company drilled a core hole over 4,000 feet deep near the city of Osseo in Hennepin County, on the west side of the St. Croix horst (Fig. 2). That drillhole, known as Osseo 75-1 or NNG 75-1, penetrated 289 feet of Quaternary material, 435 feet of Paleozoic

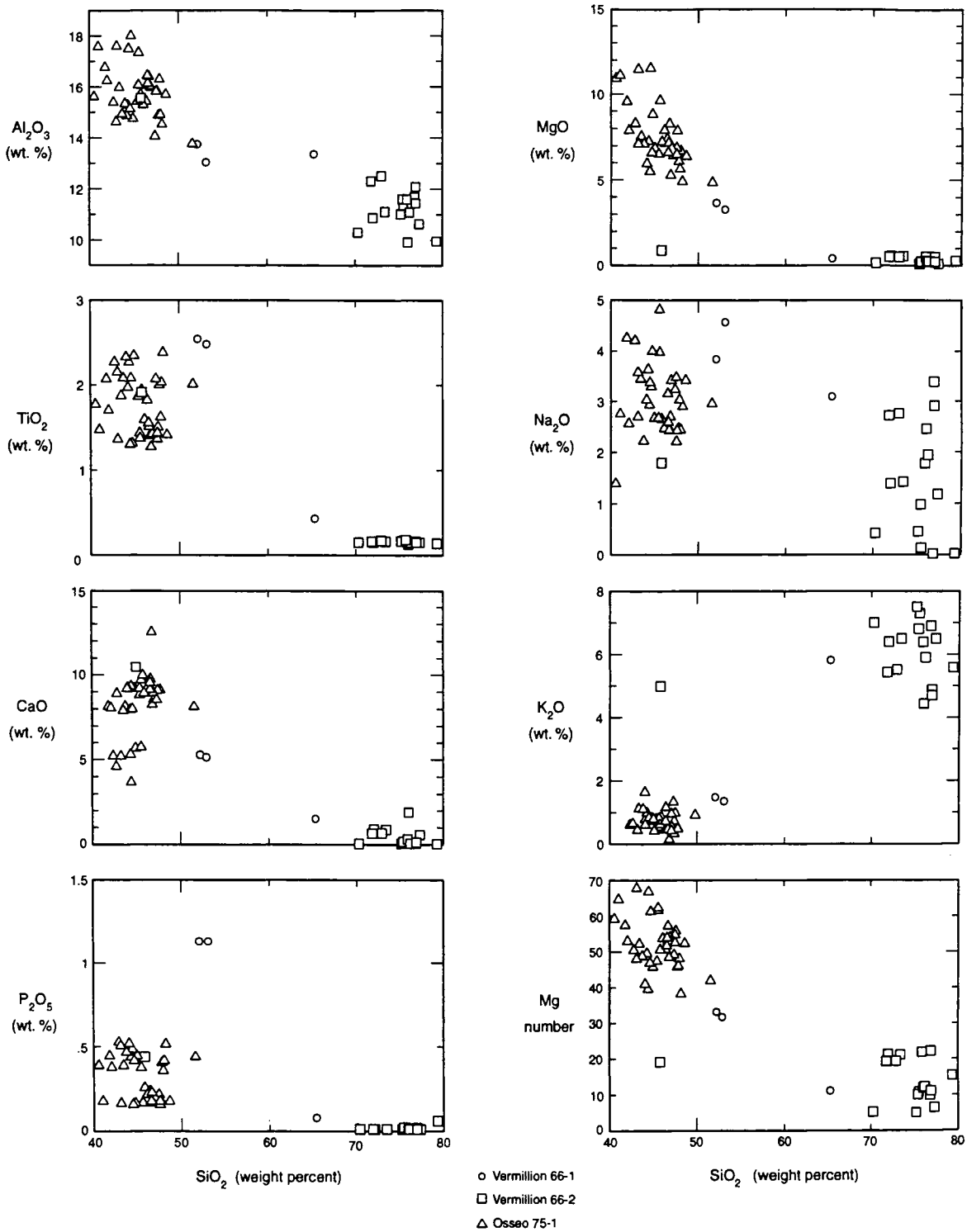

Figure 9. Major-oxide trends (Harker diagrams) of volcanic rocks from the Vermillion and Osseo areas analyzed using SiO_2 as a fractionation index. Because data exists for relatively few samples, it is not clear if the trends observed are real or whether rocks of intermediate composition simply were not sampled. The Mg number equals MgO/FeO + MgO + MnO.

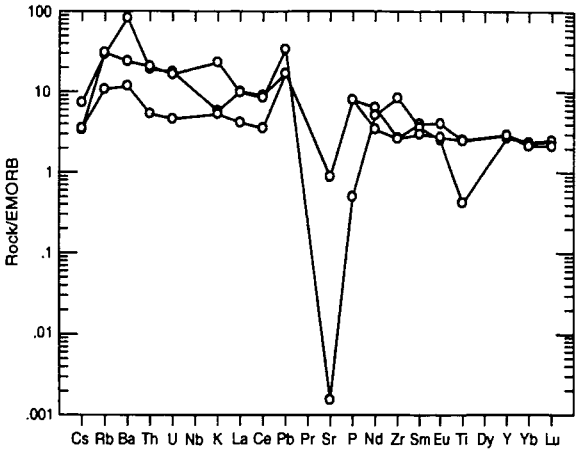

Figure 10. Spider diagrams of trace elements in volcanic rocks from Vermillion 66-1. Data are normalized against the composition of primitive mantle as determined by Sun and McDonough (1989).

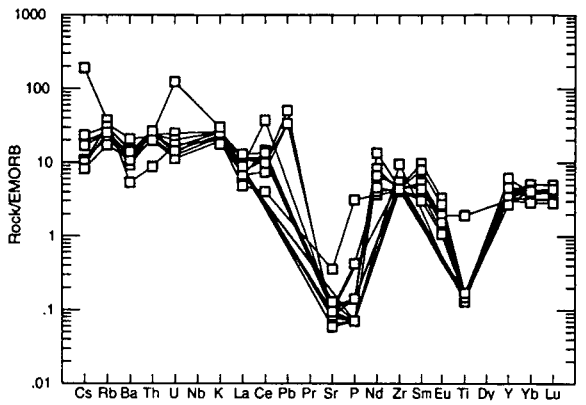

Figure 11. Spider diagrams of trace elements in volcanic rocks from Vermillion 66-2. Data are normalized against the composition of primitive mantle as determined by Sun and McDonough (1989).

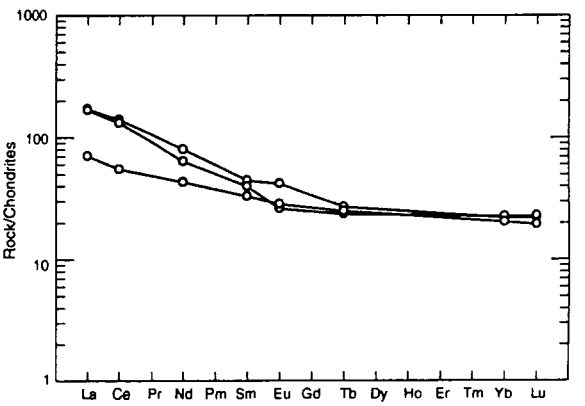

Figure 12. Rare earth element (REE) plots for volcanic rocks from Vermillion 66-1. Data are normalized against the composition of chondrite as determined by Taylor and McLennan (1985).

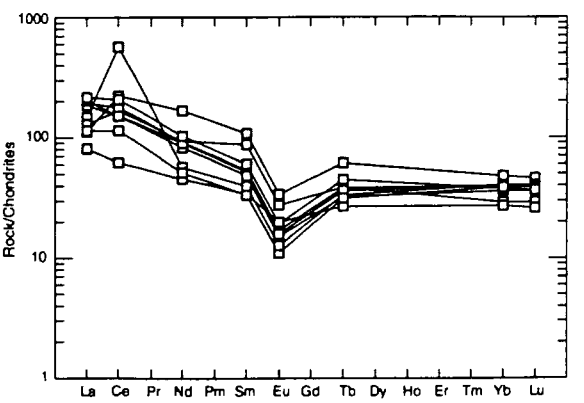

Figure 13. Rare earth element (REE) plots for volcanic rocks from Vermillion 66-2. Data are normalized against the composition of chondrite as determined by Taylor and McLennan (1985).

strata, 30 feet of lithic sandstone, siltstone, and shale presumed to represent the lower part of the Solor Church Formation, and 3,280 feet of extrusive volcanic and associated interflow sedimentary rocks (Fig. 14). Volcanic rocks make up about 90 percent of the sequences; interflow sedimentary and pyroclastic rocks make up the remainder. The volcanic component of the Osseo core was logged in considerable detail by Kurt Molenaar in the early 1980s under the auspices of the Minnesota Geological Survey. Molenaar recognized some 70 flow units, ranging in thickness from less than one to more than 532 feet, averaging 34 feet (Fig. 15). One interval, some 522-feet-thick, may either be a very thick flow or possibly a hypabyssal intrusion. Molenaar also recognized 13 substantial interflow units of sedimentary rock—including conglomerate, sandstone,

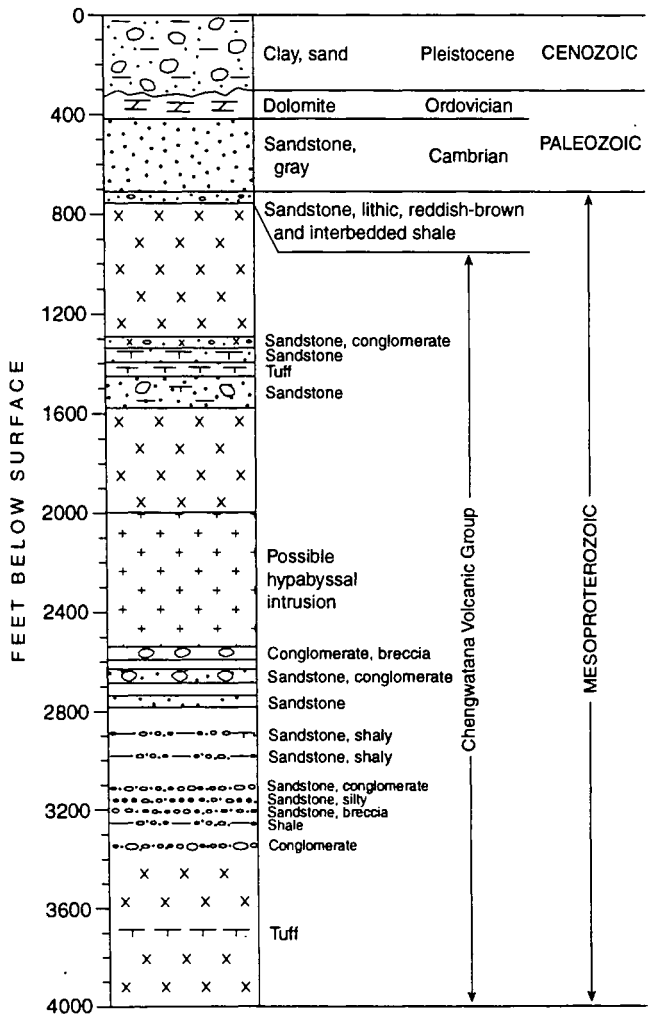

Figure 14. Schematic columnar section of strata penetrated at Osseo 75-1.

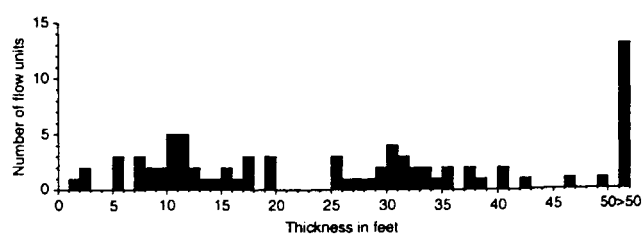

Figure 15. Histogram summarizing the thickness of individual lava flows recognized in Osseo 75-1.

siltstone and shale—ranging in thickness from less than one to 138 feet and averaging 22 feet. Lastly, he logged two pyroclastic intervals of 8- and 14-feet-thick. The interflow sedimentary rocks are scattered throughout the volcanic intersect, but both they and the pyroclastic intervals are particularly abundant between the depths of 1,300 and 1,541 feet, and between the depths of 2,535 and 2,732 feet. Very thin beds of interflow material, generally thinner than one foot, are also scattered between the depths of 2,900 and 3,300 feet.

Although no detailed mineralogical studies have been completed, the flows have primary igneous mineral assemblages (plagioclase + clinopyroxene + F-Ti oxides) and display a variety of igneous textures (ophitic, subophitic, ophimottled intergranular, intersertal, plagioclase phyric, and seriate). The textures indicate a crystallization sequence of ophimottled plagioclase → clinopyroxene → oxides, a sequence typical of tholeiitic basalt. Single flow units typically exhibit more than one texture: ophitic textures are common in the flow interior where clinopyroxene presumably had sufficient time to crystallize during slow cooling, whereas intersertal and ophimottled textures are more common at flow tops where rapid cooling prevented the growth of large clinopyroxene crystals (Wirth and others, 1996).

According to Naiman and others (1996), the upper 2,200 feet of the Osseo core is marked by metamorphic mineral assemblages that consist of calcite + epidote + chlorite + quartz + albite + oxides ± white mica. Below 2,200 feet, actinolite becomes prominent in the groundmass whereas calcite is limited to veins and amygdules. These mineral assemblages are consistent with the transition from the calcite-chlorite facies to the greenschist facies and imply that the rocks were once more deeply buried. Geochemical data for Osseo 75-1 are reported in Table 3.

Descriptive Geochemistry

Unlike the felsic rocks from the Vermillion area, the mafic rocks from Osseo 75-1 do not appear to have been metasomatically altered to any extent (Fig. 4). When classified according to SiO_2, K_2O and Na_2O contents (LeBas and others, 1986), the Osseo samples cluster within the defined fields of basalt and basanite or tephrite (Fig. 5). The mafic rocks range from alkaline to subalkaline (Fig. 6) and tend to follow tholeiitic trends toward iron enrichment in an AFM diagram (Fig. 7). On a Jensen cation plot, the analyzed samples lie within the tholeiite field (Fig. 8).

Major Oxides And Trace Elements

Major-oxide compositions of rocks from the Osseo core are illustrated in Figure 9 where SiO_2 concentrations are used as a fractionation index. Although the rocks have a restricted range of silica composition (41.01 to 51.58 wt. percent SiO_2) and display a considerable amount of scatter, the concentrations of most of the major oxides decrease with increasing silica values. Exceptions include Na_2O and K_2O, whose concentrations remain more or less constant, and CaO, whose concentration increases with increasing silica values. Figure 9 also shows that a number of the samples are fairly rich in potassium (0.65 to 0.93 wt. percent K_2O) and 12 of the 39 samples fall in a high-alumina category marked by greater than 16 wt. percent Al_2O_3.

Trace-element concentrations normalized against primitive mantle (Fig. 16) show considerable similarity, particularly in the enrichment of large-ion lithophile elements. The samples share a generally smooth, gently concave negative slope that is interrupted only by a negative thorium anomaly and a pronounced positive spike in the normalized abundance of lead. The REE plots (Fig. 17) exhibit smooth, moderately negative slopes; the light rare earth elements are enriched relative to the heavy rare earth elements. The REEs display a pattern characteristic of tholeiitic rocks from a variety of tectonic settings (Wilson, 1989). Elevated light-ion lithophile elements and lead are consistent with a petrogenesis that involved continental crustal material.

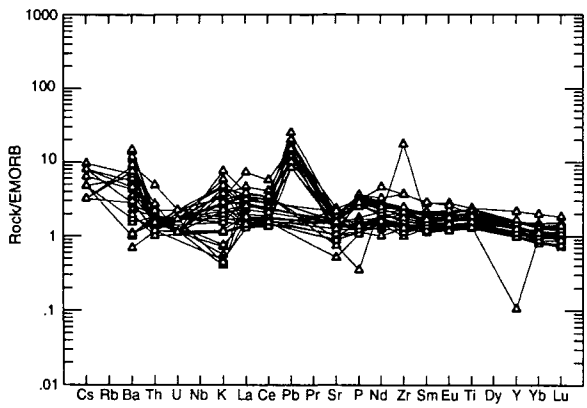

Figure 16. Spider diagrams of trace elements in volcanic rocks from Osseo 75-1. Data are normalized against the composition of primitive mantle as determined by Sun and McDonough (1989).

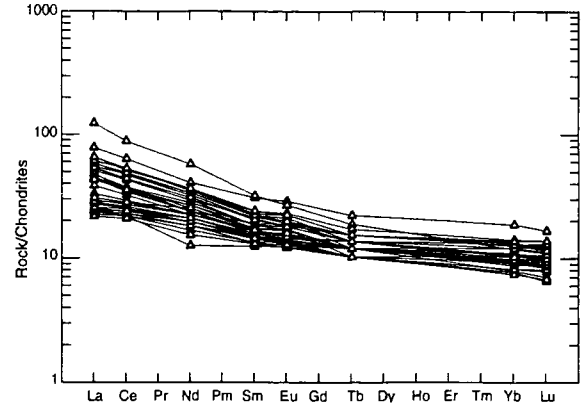

Figure 17. Rare earth element (REE) plots for volcanic rocks from Osseo 75-1. Data are normalized against the composition of chondrite as determined by Taylor and McLennan (1985).

Although no serious attempt has been made to analyze compositional changes with depth in Osseo 75-1, Figure 18 illustrates some possibly significant relationships. On the average, elemental concentrations of Al_2O_3, TiO_2, Na_2O, and MgO remain constant or increase only slightly with depth. Other major elemental constituents such as SiO_2, K_2O, and CaO remain constant or decrease slightly with depth. Ferric iron values remain more or less constant, whereas the concentration of ferrous iron appears to increase with depth. Some of the minor and trace elements have considerably different concentration patterns. For example, MnO concentrations remain relatively constant with depth whereas P_2O_5, Zr, and Ba are alternately enriched and depleted; the Ba group is abruptly enriched at a depth of about 2,500 feet. In contrast, other trace elements such as Ni and Cr exhibit similar cyclic increases and decreases, but with an abrupt decrease at a depth of 2,500 feet.

CONCLUSIONS

The chemical characteristics of the mafic flows on the St. Croix horst are similar to those of the flow sequences exposed around Lake Superior. For example, on a Jensen plot (Fig. 8), the flows in Osseo 75-1 lie within the tholeiitic field, where representative suites of basalt from the Portage Lake Volcanics (Paces, 1988), and the North Shore Volcanic Group (Basaltic Volcanism Study Project, 1981; Brannon, 1984) also plot. They are also compositionally similar to exposed parts of the Chengwatana Volcanic Group in east-central Minnesota (Wirth and others, 1996), and to mafic rocks in the pre-Phanerozoic subsurface in Kansas (Cullers and Berendsen, 1993). Pearce-Cann diagrams, which assign tectonic settings to mafic volcanic rocks on the basis of their titanium, zirconium, and yttrium (Fig. 19), show that the Osseo section plots within the "within-plate" and "ocean-floor" fields, consistent with the postulate that the volcanic rocks were extruded into a continental rift system. The mafic flow in Vermillion 66-1 plots in a similar manner.

The fact that the compositions of these various mafic sequences are broadly similar is not unexpected. The rocks of the Portage Lake Volcanics yield an average age of 1,095.1 ± 1.9 Ma (Paces, 1988; Paces and Davis, 1988). The Chengwatana Volcanic Group in east-central Minnesota yields an age of 1,094.6 ± 2.1 Ma (Zartman and others, 1997) and as such is broadly correlative

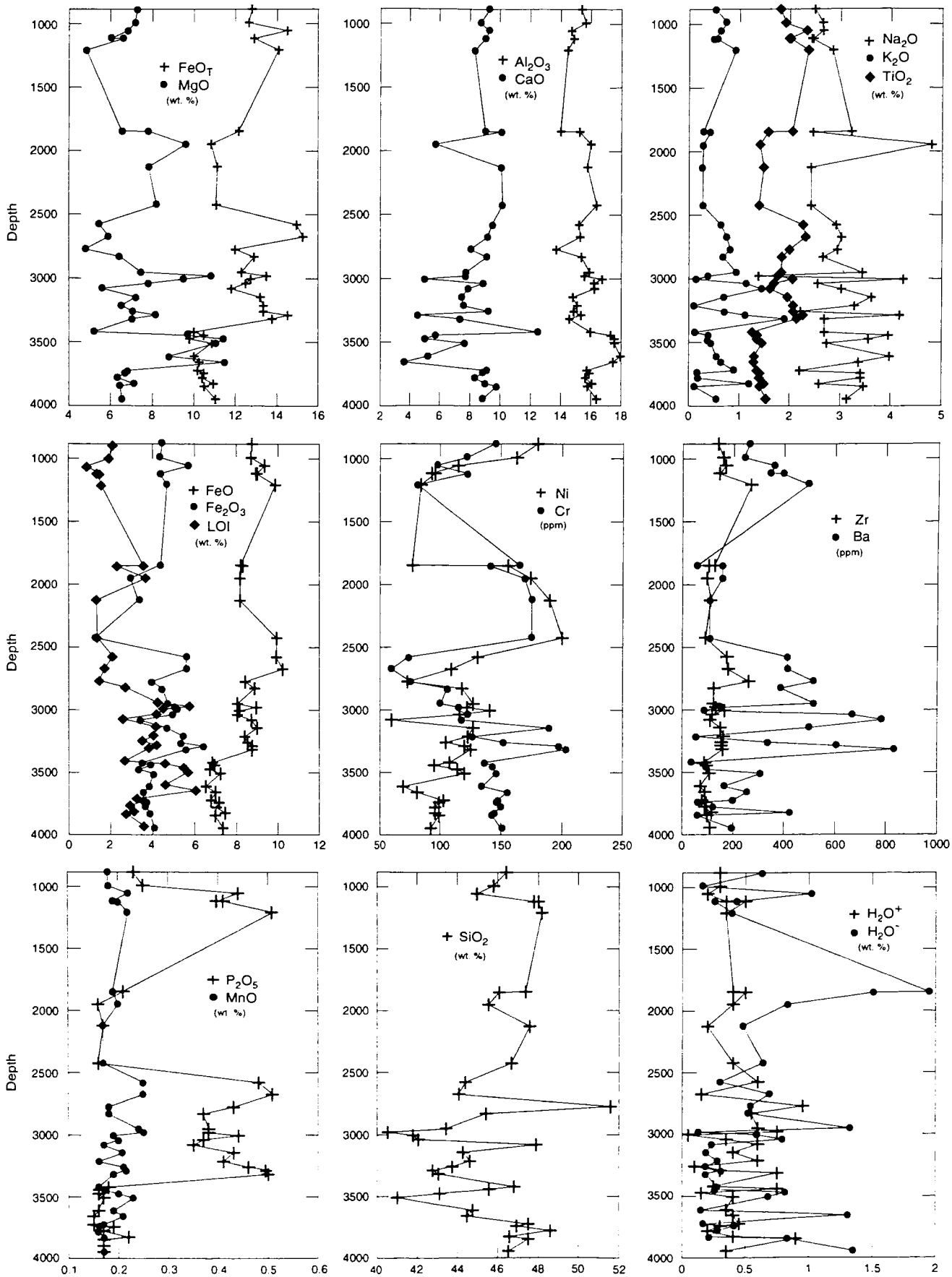

Figure 18. Plots of selected element concentrations versus depth in Osseo 75-1.

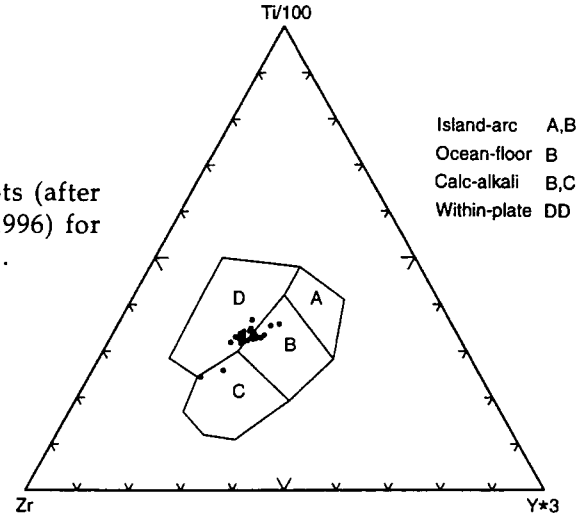

Figure 19. Immobile element plots (after Pearce and Cann, 1973; Pearce, 1996) for mafic volcanic rocks in Osseo 75-1.

with the Portage Lake Volcanics. The North Shore Volcanic Group is somewhat older, ranging in age from 1,108 to 1,098 m.y. The age of the volcanic sequence in Kansas has not been established, but it is cut by a body of gabbro thought to be a sill that yields an age of 1,097.5 ± 3 Ma (VanSchmus and others, 1990).

There are discrepancies between the stratigraphic placement and the tectonic significance of the felsic rocks in the Vermillion area. They are compositionally similar to the so-called Type I rhyolites in the Portage Lake Volcanics (Nicholson, 1992); however, one of the rhyolite flows from Vermillion 66-2 has a zircon age of around 1,130 m.y. (Zartman and others, 1997), an age some 35 m.y. older than that of the Portage Lake Volcanics.

Two possible explanations for this discrepancy exist. First, the dated zircon grains from Vermillion 66-2 may have been inherited from older crust beneath the rift-related sequence and therefore the measured age does not reflect the time when the flow actually erupted. However, the zircon grains appear to be fresh and pristine, and generally lack the textural attributes associated with inherited grains. Second, the rhyolitic rocks could be part of an older volcanic sequence as yet not recognized anywhere else in the rift system. If so, the formation of the two rhyolite sequences implies similar petrogenetic processes that must have been repeated in both space and time. According to Nicholson (1992), that petrogenesis involved the partial melting of older, Midcontinent rift-related rocks and subsequent emplacement of the partial melt in the distal parts of the central volcanic complexes of mafic composition.

Table 1. Major-oxide, trace element and CIPW normative compositions for selected samples from drill hole Vermillion 66-1, Dakota County, Minnesota. See Figure 4 for approximate sample depths.

Major oxide and trace element analyses by XRF methods conducted by Analytical Geochemistry Laboratories, Department of Geology and Geophysics, University of Minnesota.

INAA analyses conducted by Johnson Space Center, Houston, Texas.

(n.d.) not determined; (-) below detection limit

sample	A1	A2	A3	A4	A5
Major-oxides (in weight percent)					
SiO_2	52.20		65.4		53.20
TiO_2	2.53		0.42		2.47
Al_2O_3	13.70		13.32		13.00
Fe_2O_3	2.50		1.00		2.80
FeO	10.60		3.90		10.10
MnO	0.59		0.30		0.56
MgO	3.60		0.33		3.20
CaO	5.27		1.45		5.04
Na_2O	3.82		3.08		4.54
K_2O	1.45		5.79		1.32
P_2O_5	1.12		0.07		1.12
H_2O^+	n.d.		n.d.		n.d.
H_2O^-	n.d.		n.d.		n.d.
CO_2	0.13		0.11		0.40
LOI	2.5		0.6		1.9
Subtotal	100.01		95.77		99.65
X-ray fluorescence (XRF) in parts per million					
Be	1.4		0.5		1.3
Zn	401		36.1		324
Cu	47		197		55.7
Sc	38		11.5		37
Co	46		8		39
Pb	10		20		10
Ni	11.1		5.0		9.5
Cr	12		6		10.3
Rb	62		133		52
V	134		-		128
Zr	194		608		189
Y	65		59		64

Table 1. continued

sample	A1	A2	A3	A4	A5
Instrumental Neutron Activation Analysis (INAA) in parts per million					
Cs	0.46	0.701	0.213	0.323	0.22
Rb	148	69.0	154	117	53.8
Ba	4710	598	1359	1009	669
Th	11.39	3.47	12.38	9.87	3.19
U	3.17	0.85	2.95	2.4	0.82
Ta	1.64	.805	1.70	1.48	0.83
Sr	134	-	0.24	-	137
Hf	13.61	5.07	14.70	12.46	5.00
As	10.9	4.4	2.51	6.03	4.7
Rare earth elements (in parts per million)					
La	62.9	30.1	61.5	71.2	25.9
Ce	134.1	67.7	126	141.6	52.7
Nd	57	35	45.4	51	30.7
Sm	10.29	8.65	9.21	9.55	7.64
Eu	3.64	2.64	2.27	2.93	2.48
Tb	1.57	1.57	1.37	1.36	1.45
Yb	5.49	5.26	5.62	4.89	5.06
Lu	0.836	0.781	0.872	0.744	0.742
CIPW (in weight percent)					
%AN	33.05		17.22		22.57
Q	5.17		20.39		4.85
Or	8.80		36.00		8.01
Ab	33.19		27.42		39.46
An	16.38		5.70		11.50
Ne					
C					
Di	2.48		1.21		5.61
Hy	22.66		6.75		18.91
Wo					
Ol					
Ac					
Mt	3.72		1.53		4.17
Il	4.93		0.84		4.82
Hem					
Ti					
Ap	2.66		0.17		2.67

Table 2. Major oxide, trace element and CIPW normative compositions for selected samples from drill hole Vermillion 66-2, Dakota County, Minnesota. See Figure 4 for approximate sample depths.

Major oxide and trace element analyses by XRF methods conducted by Analytical Geochemistry Laboratories, Department of Geology and Geophysics, University of Minnesota.

INAA analyses conducted by Johnson Space Center, Houston, Texas.

(n.d.) not determined; (-) below detection limit

sample	1B	1C	2B	3B[1]	3B[2]	4B	4C	5B	5C[1]	5C[2]
Major-oxides (in weight percent)										
SiO_2		75.50	79.30	75.20	70.30		76.80	75.40	73.40	72.0
TiO_2		0.17	0.14	0.16	0.15		0.16	0.16	0.16	0.15
Al_2O_3		11.32	9.95	11.00	10.30		11.68	11.59	11.10	10.86
Fe_2O_3		2.10	1.40	1.60	1.60		2.30	1.20	1.40	1.30
FeO		1.80	1.30	2.30	2.40		1.20	2.60	2.40	2.40
MnO		0.05	0.06	0.06	0.05		0.04	0.04	0.06	0.07
MgO		0.25	0.26	0.11	0.12		0.20	0.23	0.55	0.54
CaO		0.11	0.01	0.05	0.04		0.05	0.15	0.88	0.86
Na_2O		0.13	0.02	0.45	0.42		0.02	0.98	1.42	1.39
K_2O		7.30	5.58	7.50	7.0		6.9	6.80	6.50	6.40
P_2O_5		0.02	0.06	0.01	0.01		0.02	0.02	0.01	0.01
H_2O^+		1.0	n.d.	n.d.	n.d.		n.d.	n.d.	n.d.	n.d.
H_2O^-		n.d.	n.d.	n.d.	n.d.		n.d.	n.d.	n.d.	n.d.
CO_2		0.01	0.01	0.01	0.01		0.003	0.15	1.22	n.d.
LOI		1.00	1.50	n.d.	0.70		1.50	0.90	0.90	0.80
Subtotal		100.76	99.59	98.45	93.10		100.87	100.22	100.00	96.78
X-ray fluorescence (XRF) in parts per million										
Be		1.1	1.46	1.50	1.39		2.00	2.31		1.82
Zn		36.7	45.0	37.0	34.2		17.8	30.0	16.0	15.9
Cu		36.2	51.3	28.4	26.5		63	23.2	19.0	20.0
Sc		2.7	2.5	2.5	2.3		2.5	2.2	3.0	2.9
Co		5.2	<0.1	0.1	0.1		1.5	0.1	0.1	0.1
Pb		<20	<20	<20	<20		<10	<20	<20	<20
Ni		5.0	7.6	37	34.3		6.1	10.8	4.0	4.8
Cr		3.4		3.3	3.1		1.0	6.0	4.0	4.0
Rb		127	128	100	93		146	140	122	120
V		10	16	9	8		14	13		15
Zr		334	298	325	304		374	353	328	322
Y		90	59	77	72		96	87	91	89

Table 2. continued

sample	5D	5E	5F	5G[1]	5G[2]	5H	6B	6C	7B	7C	7D
Major oxides (in weight percent)											
SiO_2	75.90	77.30	76.90	72.90	71.80	76.00	45.80		76.20		76.90
TiO_2	0.16	0.15	0.15	0.17	0.16	0.13	1.91		0.15		0.15
Al_2O_3	11.58	10.62	11.44	12.50	12.30	9.92	15.56		11.08		12.08
Fe_2O_3	1.40	0.90	1.10	4.21	0.90	1.30	6.80		1.40		1.10
FeO	2.0	2.30	2.20	n.d.	3.00	2.40	0.60		2.20		2.30
MnO	0.03	0.04	0.03	-	-	0.06	0.26		0.05		0.07
MgO	0.51	0.12	0.51	0.51	0.51	0.27	0.89		0.27		0.23
CaO	0.29	0.57	0.06	0.67	0.66	1.90	10.48		0.05		0.12
Na_2O	1.78	1.18	2.91	2.76	2.72	2.45	1.8		1.94		3.39
K_2O	6.39	6.50	4.88	5.51	5.43	4.44	4.99		5.90		4.70
P_2O_5	0.01	0.01	0.02	<0.01	0.01	0.01	0.44		<0.01		0.01
H_2O^+	n.d.	n.d.	n.d.	n.d.	n.d.	n.d.	n.d.		n.d.		n.d.
H_2O^-	n.d.	n.d.	n.d.	n.d.	n.d.	n.d.	n.d.		n.d.		n.d.
CO_2	0.21	0.31	0.03	n.d.	0.49	1.38	7.66		0.03		0.07
LOI	0.50	0.50	0.70	n.d.	0.60	0.50	2.40		0.50		0.40
Subtotal	100.76	100.50	100.93	99.23	98.58	100.76	99.59		99.77		101.52
X-ray fluorescence (XRF) in parts per million											
Be	1.96	11.1	4.47		3.37	1.42	13.3		1.62		1.87
Zn	15.5	16.1	23.5	14.0	13.8	15.5	124		12.5		22
Cu	19.4	19.8	27.9	31.6	31.1	73.4	376		32.3		34.3
Sc	2.8	2.4	1.7	<1.0	2.8	2.2	28.1		2.0		1.9
Co	0.1	2.0	1.4	<0.1	5.0	1.0	19		1.1		4.0
Pb	30	20	<10	<10	<20	<10	<10		20		<10
Ni	5.6	5.7	4.2	<4.0	7.0	6.0	26.4		6.3		6.2
Cr	4.0	6.0	3.7	<3.0	4.1	7.0	25		4.7		4.9
Rb	137	146	105	164	162	92	185		149		108
V	6	5.0	1.3	<0.6	0.6	7.2	185		10		8
Zr	360	327	312	402	396	691	303		318		315
Y	85	80	135	101	100	81	68		75		100

Table 2. continued

sample	1B	1C	2B	3B[1]	3B[2]	4B	4C	5B	5C[1]	5C[2]
Instrumental Neutron Activation Analysis (INAA) in parts per million										
Cs	0.638	1.21	1.07	0.685		1.12			0.578	
Rb	130.0	130.0	124.9	108.3		128.0			128.0	
Ba	448	635.0	523.0	598.0		600.0			737.0	
Th	15.91	14.93	12.66	14.47		14.43			14.04	
U	4.33	2.38	2.23	22.0		4.70			4.43	
Ta	n.d.	n.d.	n.d.	2.53	n.d.	n.d.	n.d.	n.d.	n.d.	n.d.
Sr	25.0	15.7	16.0	15.0	9.20	15.0	13.00	12.90	20.00	12.20
Hf	12.71	12.71	10.58	11.85		13.25			12.04	
As	3.5	3.40	2.62	47.0		4.7			14.9	
Rare earth elements (in parts per million)										
La	138.8	41.3	54.8	47.8		16.06			72.1	
Ce	370.0	214.9	549	161.4		26.3			171.7	
Nd	120.0	120.0	40.9	67.0		11.6			66.0	
Sm	25.3	25.3	9.28	20.5		3.52			12.58	
Eu	2.99	2.99	1.12	2.44		0.57			1.50	
Tb	3.62	3.62	1.98	2.28		1.58			2.26	
Yb	11.94	11.94	10.09	7.26		9.33			9.94	
Lu	1.77	1.77	1.54	1.12		1.48			1.54	
CIPW (in weight percent)										
%AN		27.39		4.58	3.61		40.96	6.89	26.36	26.32
Q		46.20	58.20	43.05	42.75		50.19	41.78	36.96	36.82
Or		43.69	33.62	45.03	44.78		41.04	40.52	39.25	39.41
Ab		1.11	0.17	3.87	3.85		0.17	8.36	12.28	12.25
An		0.42	0.35	0.19	0.14		0.12	0.62	4.39	4.38
Ne										
C		3.09	4.08	2.11	2.15		4.16	2.41	0.16	0.11
Di										
Hy		2.03	1.79	3.07	3.50		0.62	4.20	4.56	4.75
Wo										
Ol										
Ac										
Mt		3.08	2.07	2.36	2.51		3.36	1.75	2.07	1.96
Il		0.33	0.27	0.31	0.31		0.31	0.31	0.31	0.30
Hem										
Ti										
Ap		0.05	0.14	0.02	0.03		0.05	0.05	0.02	0.02

Table 2. continued

sample	5D	5E	5F	5G[1]	5G[2]	5H	6B	6C	7B	7C	7D
Instrumental Neutron Activation Analysis (INAA) in parts per million											
Cs	0.623	0.637	0.516				12.08	7.38	1.48	0.734	
Rb	168.0	154.0	86.8				189.0	301.0	154.0	116.1	
Ba	1179.0	830.0	614.0				305.0	446.0	796.	608.0	
Th	13.38	14.27	11.89				5.24	4.49	15.90	13.46	
U	2.89	3.59	2.01				3.10	5.54	2.56	2.38	
Ta	n.d.	n.d.	n.d.				1.08	-	2.54	-	
Sr	10.00	13.00	17.5	14.9	14.7	n.d.	55	36.0	<13.0	10.0	
Hf	11.83	11.90	10.06				7.46	6.37	11.81	11.71	
As	5.10	6.20	9.30				5.1	3.6	4.59	4.6	
Rare earth elements (in parts per million)											
La	69.0	75.5	80.2				30.2	20.31	42.5	66.8	
Ce	145.8	146.1	200.3				60.2	51.6	110.5	151.1	
Nd	59.6	64.6	74.0				32.8	25.6	36.9	58.1	
Sm	11.36	12.17	14.1				7.98	7.65	7.84	11.11	
Eu	1.33	1.40	1.71				1.76	1.55	0.97	1.27	
Tb	1.91	2.14	2.64				1.59	1.57	1.86	2.19	
Yb	8.97	10.00	9.40				6.76	5.62	9.64	9.26	
Lu	1.39	1.55	1.41				1.0	0.84	1.50	1.41	
CIPW (in weight percent)											
%AN	8.72	21.67	0.67	12.46	12.24	12.49	56.32		1.49		2.03
Q	38.64	42.81	39.05	33.82	31.80	40.68	0.06		40.89		36.75
Or	37.74	38.53	28.78	32.82	32.92	26.54	32.94		35.13		27.49
Ab	15.05	10.02	24.57	23.54	23.61	20.97	17.01		16.54		28.39
An	1.44	2.77	0.17	3.35	3.29	2.99	21.94		0.25		0.59
Ne											
C	1.21	0.63	1.31	0.78	0.79				1.42		1.19
Di						5.62	5.34				
Hy	3.58	3.62	4.20	1.28	5.92	1.03			3.43		3.73
Wo							9.34				
Ol											
Ac											
Mt	2.03	1.31	1.59		1.34	1.91			2.05		1.58
Il	0.30	0.29	0.28		0.31	0.25	2.04		0.29		0.28
Hem				4.24			7.60				
Ti							2.60				
Ap		0.02	0.05		0.02	0.02	1.14				

Table 3. Major oxide, trace element and CIPW normative compositions for selected samples from drill hole Osseo 75-1, Hennepin County, Minnesota. See Figure 15 for sample depths.

Analyses conducted by Activation Laboratories Limited, Ancoster, Ontario.

sample depth	882	990	1054	1114A	1114B	1208	1846	1850	1948	2125	2425	2579
Major oxides (in weight percent)												
SiO_2	46.43	45.80	44.97	47.77	48.00	48.18	47.39	46.08	45.56	47.59	46.68	44.40
TiO_2	1.81	1.92	2.34	1.99	2.02	2.37	2.06	1.58	1.42	1.49	1.39	2.26
Al_2O_3	15.37	15.65	14.69	14.82	14.85	14.47	14.01	15.24	16.01	15.78	16.35	15.21
Fe_2O_3	4.47	4.38	5.73	4.37	4.36	4.68	4.39	4.28	2.95	3.32	1.27	5.60
FeO	8.75	8.70	9.35	9.00	8.97	9.87	8.22	8.31	8.17	8.16	9.93	9.92
MnO	0.18	0.18	0.22	0.19	0.20	0.22	0.19	0.19	0.20	0.17	0.17	0.25
MgO	7.26	7.17	6.80	6.05	6.64	4.83	6.54	7.85	9.64	7.83	8.22	5.46
CaO	9.33	8.73	9.29	9.07	9.05	8.34	9.02	10.05	5.77	10.09	10.18	9.48
Na_2O	2.49	2.64	2.66	2.46	2.43	2.85	3.22	2.46	4.80	2.42	2.42	2.92
K_2O	0.53	0.75	0.65	0.49	0.55	0.93	0.30	0.43	0.29	0.28	0.28	0.64
P_2O_5	0.23	0.25	0.44	0.40	0.41	0.51	0.21	0.21	0.16	0.17	0.16	0.48
H_2O^+	0.30	0.30	0.20	0.35	0.50	0.35	0.40	0.50	0.40	0.20	0.40	0.60
H_2O^-	0.64	0.16	1.02	0.43	0.26	0.40	1.95	1.51	0.83	0.48	0.64	0.30
CO_2	<0.01	0.03	0.06	0.06	<0.01	0.06	0.35	0.06	0.32	<0.01	0.03	0.44
LOI	2.12	1.96	0.93	1.49	1.39	1.60	3.45	2.29	3.58	1.37	1.39	2.10
Subtotal	99.91	98.62	99.35	98.94	99.63	99.66	101.70	101.04	100.10	99.35	99.51	100.06
X-ray fluorescence (XRF) in parts per million												
Be	<2.0	<2.0	<2.0	<2.0	<2.0	<2.0	<2.0	<2.0	<2.0	<2.0	<2	<2
Zn	105	107	123	94	104	122	146	92	98	96	86	134
Cu	155	142	111	103	108	132	339	102	11	116	121	119
Sc	27.0	26.5	30.6	31.8	32.1	30.5	36.6	29.4	27.3	27.7	26.1	28.3
Co	52.0	52.5	51.5	42.8	45.9	41.0	47.9	55.3	52.9	51.1	53.5	52.3
Pb	<5	<5	9	<5	<5	10	8	<5	8	8	5	8
Ni	180	163	115	93	96	84	77	156	174	190	200	131
Cr	145	122	97.0	123	122	81.5	165	141	169	175	175	72.8
Rb	13	<10	18	<10	<10	<10	<10	<10	<10	<10	<10	16
V	172	172	199	207	209	175	227	170	90	155	155	220
Zr	141	161	168	150	144	270	128	106	98	110	93	176
Y	27	29	35	30	30	47	29	24	22	22	21	35

Table 3. continued

sample depth	2675	2774	2829	2951	2980	3004	3038	3078	3144	3213	3257	3288
Major oxides (in weight percent)												
SiO_2	44.07	51.58	45.43	43.44	40.56	41.81	42.05	47.90	44.28	44.63	43.75	42.78
TiO_2	2.32	2.00	1.85	1.84	1.76	2.06	1.69	1.61	1.96	2.07	2.07	2.26
Al_2O_3	15.28	13.7	15.37	15.92	15.56	16.71	16.19	16.23	14.80	15.08	14.86	15.34
Fe_2O_3	5.59	3.97	4.46	4.73	5.04	5.11	4.94	3.40	4.68	5.50	5.34	6.41
FeO	10.23	8.41	8.88	8.04	8.95	8.14	8.04	8.74	9.00	8.39	8.55	8.77
MnO	0.25	0.18	0.18	0.24	0.25	0.19	0.20	0.17	0.21	0.16	0.21	0.21
MgO	5.91	4.80	6.46	7.48	10.87	9.53	7.82	5.60	7.21	6.54	7.06	8.22
CaO	9.17	8.05	9.16	7.75	7.74	5.05	8.86	7.91	7.45	7.54	9.25	4.53
Na_2O	3.02	2.94	2.66	3.43	1.38	4.24	2.55	3.02	3.62	3.28	2.21	4.17
K_2O	0.75	0.82	0.68	0.94	0.38	0.14	1.14	1.45	0.7	0.10	0.71	1.12
P_2O_5	0.51	0.43	0.37	0.38	0.38	0.44	0.37	0.35	0.43	0.41	0.46	0.49
H_2O^+	0.15	0.95	0.55	0.60	0.75	0.05	0.35	0.60	0.40	0.60	0.10	0.30
H_2O^-	0.69	0.54	0.52	1.32	0.13	0.59	0.79	0.24	0.19	0.28	0.19	0.31
CO_2	0.54	0.09	0.66	0.92	0.06	0.06	0.28	0.25	0.87	0.03	0.19	0.09
LOI	1.73	1.48	2.67	4.11	5.52	4.35	4.06	2.57	4.06	3.92	3.42	4.05
Subtotal	100.21	99.94	99.90	100.14	99.33	98.47	99.33	100.04	99.86	98.53	98.37	99.05
X-ray fluorescence (XRF) in parts per million												
Be	<2	<2	<2	<2	<2	<2	<2	<2	<2	<2	<2	<2
Zn	141	134	11.6	128	206	160	120	100	128	119	133	148
Cu	64	93	116	69	43	11	3	109	64	127	32	23
Sc	27.8	24.3	29.3	29.3	29.6	33.4	26.5	26.6	28.9	28.5	28.3	30.5
Co	56.2	37.3	50.9	54.0	85.7	80.4	51.4	47.2	62.9	59.8	58.9	59.2
Pb	15	10	6	5	11	7	12	<5	<5	<5	<5	<5
Ni	109	73	118	127	122	141	116	60	127	123	105	120
Cr	59.9	75.4	106	101	116	116	123	118	189	127	153	198
Rb	14	12	15	<10	<10	12	20	31	<10	<10	19	20
V	202	202	193	187	187	162	180	167	184	201	191	203
Zr	178	264	126	127	133	166	120	111	152	164	154	163
Y	35	36	30	30	29	34	28	27	32	33	32	34

Table 3. continued

sample depth	3315	3420	3444	3473	3508	3611	3658	3724	3743	3781	3826	3847	3945
Major oxides (in weight percent)													
SiO_2	43.09	46.80	45.59	43.13	41.01	44.74	44.48	47.51	46.93	48.61	46.59	47.51	46.53
TiO_2	2.14	1.26	1.36	1.35	1.46	1.30	1.29	1.35	1.41	1.40	1.50	1.42	1.54
Al_2O_3	14.56	15.97	17.28	17.55	17.53	17.94	17.45	15.73	15.91	15.64	16.07	15.76	16.38
Fe_2O_3	5.57	3.48	3.90	3.38	4.04	3.84	3.60	3.74	3.68	3.72	3.89	3.90	4.08
FeO	8.75	6.86	6.95	6.74	7.24	6.55	7.01	6.80	7.16	7.05	7.45	6.99	7.35
MnO	0.19	0.16	0.17	0.20	0.23	0.19	0.21	0.17	0.16	0.16	0.17	0.17	0.17
MgO	7.06	5.22	9.60	11.42	11.06	8.80	11.47	6.83	6.70	6.34	7.11	6.45	6.54
CaO	7.38	12.46	5.70	5.02	7.61	5.21	3.61	9.13	8.87	8.31	9.06	9.79	8.88
Na_2O	2.68	2.69	3.96	3.56	2.74	3.98	3.36	2.20	3.40	3.40	2.58	3.46	3.14
K_2O	1.90	0.12	0.39	0.38	0.44	0.55	0.65	0.90	0.18	0.19	1.20	0.11	0.56
P_2O_5	0.50	0.18	0.16	0.16	0.17	0.16	0.15	0.15	0.19	0.17	0.22	0.17	0.17
H_2O^+	0.75	0.25	0.75	0.15	0.40	0.35	0.40	0.45	0.30	0.20	0.40	0.90	0.35
H_2O^-	0.19	0.27	0.26	0.81	0.68	0.15	1.30	0.17	0.41	0.28	0.21	0.83	1.35
CO_2	0.59	0.09	0.03	0.03	0.12	<0.01	0.03	0.03	<0.01	0.06	0.03	<0.01	<0.01
LOI	3.73	2.63	4.43	5.26	5.44	4.44	5.80	3.16	3.45	2.87	3.04	2.70	3.48
Subtotal	99.08	98.44	100.53	99.14	100.17	98.20	100.81	98.32	98.75	98.40	99.52	100.16	100.52
X-ray fluorescence (XRF) in parts per million													
Be	<2	<2	<2	<2	<2	<2	<2	<2	<2	<2	<2	<2	<2
Zn	123	55	114	149	137	128	157	84	87	91	93	79	88
Cu	91	53	42	86	88	51	61	340	96	111	144	117	140
Sc	29.9	26.8	29.1	29.5	30.6	28.4	28.1	29.8	30.4	31.4	30.6	30.5	31.7
Co	60.3	40.2	55.1	73.8	70.4	53.5	59.8	50.2	51.9	48.8	49.4	48.5	49.7
Pb	<5	<5	<5	<5	<5	<5	<5	<5	<5	7	<5	<5	<5
Ni	125	108	95	114	120	69	81	103	99	96	96	99	92
Cr	203	136	143	144	146	135	155	147	146	149	145	143	150
Rb	54	<10	<10	15	<10	10	13	22	<10	<10	20	<10	16
V	204	173	161	137	173	162	195	176	181	186	193	178	178
Zr	161	88	95	95	107	72	90	80	97	94	118	101	111
Y	33	21	23	23	25	23	23	23	25	25	25	24	27

Table 3. continued

sample depth	882	990	1054	1114A	1114B	1208	1846	1850	1948	2125	2425	2579
Instrumental Neutron Activation Analysis (INAA) in parts per million												
Cs	<0.2	0.4	<0.2	0.3	0.6	0.2	<0.2	0.5	0.2	<0.2	<0.2	<0.2
Ba	264	243	362	348	390	497	62	157	159	109	107	413
Th	1.1	1.2	0.9	0.9	0.9	1.6	1.0	0.7	0.7	0.6	0.7	0.9
U	0.2	0.2	<0.1	<0.1	0.3	0.2	0.2	0.3	<0.1	<0.1	0.2	<0.1
Ta	0.4	0.6	0.8	0.3	<0.3	0.5	<0.3	<0.3	0.6	<0.3	0.5	0.6
Sr	228	228	230	234	228	251	151	190	326	222	224	280
Hf	2.7	3.2	3.2	2.8	2.8	5.2	2.7	2.5	2.1	2.0	2.1	3.5
As	<1	<1	<1	<1	<1	<1	<1	<1	<1	<1	<1	<1
Rare earth elements (in parts per million)												
La	14.2	16.0	18.8	16.1	16.4	28.9	12.2	10.5	8.8	8.7	8.3	24.1
Ce	31	35	41	36	36	61	28	24	21	21	21	51
Nd	16	19	21	17	20	29	16	14	12	13	9	25
Sm	3.96	4.30	4.93	4.37	4.32	7.13	3.93	3.43	3.11	3.09	2.89	5.28
Eu	1.47	1.49	1.75	1.66	1.56	2.51	1.32	1.21	1.20	1.11	1.08	1.94
Tb	0.7	0.7	0.7	0.8	0.8	1.3	0.8	0.6	0.6	0.7	0.6	0.9
Yb	2.28	2.37	3.01	2.65	2.68	4.66	2.44	2.05	1.93	1.98	1.86	3.33
Lu	0.32	0.33	0.43	0.38	0.38	0.64	0.34	0.30	0.25	0.27	0.26	0.46
CIPW (in weight percent)												
%AN	58.08	56.18	53.81	57.31	57.65	49.82	45.65	58.44	40.53	60.50	61.65	51.76
Q				2.93	2.25	2.63						
Or	3.23	4.61	3.95	3.00	3.33	5.65	1.86	2.63	1.80	1.70	1.71	3.91
Ab	21.76	23.23	23.17	21.55	21.09	24.80	28.52	21.53	32.89	21.05	21.10	25.57
An	30.15	29.78	27.00	28.93	28.71	24.62	23.96	30.28	22.41	32.24	33.93	27.43
Ne									5.35			
C												
Di	13.06	11.00	14.18	12.20	11.88	11.95	17.38	16.08	5.35	14.64	13.96	14.76
Hy	17.44	13.14	11.50	19.97	21.34	17.53	15.98	12.18		18.93	9.07	5.64
Wo												
Ol	3.58	7.25	6.02				1.05	7.28	24.46	3.18	15.25	8.69
Ac												
Mt	6.69	6.60	8.55	6.56	6.49	6.98	6.66	6.42	4.50	4.95	1.90	8.40
Il	3.55	3.79	4.58	3.91	3.94	4.63	4.09	3.10	2.84	2.91	2.72	4.44
Hem												
It												
Ap	0.55	0.60	1.05	0.96	0.97	1.22	0.51	0.50	0.39	0.40	0.38	1.15

Table 3. continued

sample depth	2675	2774	2829	2951	2980	3004	3038	3078	3144	3213	3257	3288
Instrumental Neutron Activation Analysis (INAA) in parts per million												
Cs	<0.2	<0.2	<0.2	<0.2	<0.2	<0.2	<0.2	<0.2	<0.2	0.3	<0.2	<0.2
Ba	413	516	387	521	152	86	663	787	500	56	338	612
Th	0.9	2.9	0.7	0.7	1.1	1.1	0.8	1.1	1.1	1.2	1.0	1.1
U	0.2	0.4	<0.1	<0.1	<0.1	<0.1	<0.1	0.3	0.3	<0.1	0.3	0.2
Ta	0.8	1.0	0.4	0.7	0.4	0.4	0.6	0.8	0.6	0.8	0.8	0.4
Sr	294	362	239	202	276	169	260	256	247	328	237	114
Hf	3.4	5.1	2.6	2.5	2.8	3.2	2.3	2.8	3.3	3.2	3.3	3.7
As	<1	<1	<1	<1	2	1	<1	<1	1	1	<1	1
Rare earth elements (in parts per million)												
La	24.2	45.5	17.4	17.7	19.7	21.6	16.2	15.8	20.3	19.8	21.4	22.5
Ce	49	85	36	34	41	45	33	34	46	42	47	51
Nd	26	41	18	17	21	23	17	19	24	22	24	25
Sm	5.13	7.42	4.01	3.83	4.29	4.83	3.62	4.02	5.05	4.71	5.17	5.52
Eu	1.84	2.34	1.48	1.38	1.46	1.59	1.39	1.49	1.67	1.56	1.73	2.01
Tb	0.8	1.1	0.6	0.7	0.7	0.9	0.7	0.7	0.9	0.8	0.9	1.0
Yb	3.25	2.95	2.62	2.56	2.76	3.19	2.46	2.71	3.16	3.01	3.20	3.52
Lu	0.45	0.42	0.37	0.35	0.39	0.44	0.34	0.40	0.49	0.48	0.50	0.53
CIPW (in weight percent)												
%AN	50.36	46.66	55.43	50.49	75.06	41.01	61.55	50.86	42.78	48.49	60.41	40.66
Q		7.51										
Or	4.56	5.00	4.21	5.90	2.42	0.89	7.18	8.89	4.39	0.63	4.44	7.05
Ab	26.32	25.68	23.57	26.31	12.57	34.16	19.54	26.51	31.29	29.62	19.80	30.83
An	26.70	22.47	29.31	26.83	37.84	23.74	31.29	27.44	23.39	27.89	30.20	21.13
Ne				2.44		2.30	1.87		0.64			3.66
C						1.56						
Di	13.70	13.01	12.82	9.17	0.67		10.46	8.95	10.40	7.42	12.28	1.99
Hy	1.19	15.44	12.80		20.40			12.78		17.23	15.55	
Wo												
Ol	13.44		5.95	17.44	13.68	24.15	17.70	6.30	17.71	3.49	4.24	20.74
Ac												
Mt	8.35	5.94	6.77	7.28	7.87	7.93	7.63	5.11	7.19	8.51	8.20	9.90
Il	4.54	3.92	3.68	3.71	3.60	4.19	3.42	3.17	3.95	4.20	4.16	4.57
Hem												
It												
Ap	1.22	1.03	0.90	0.93	0.95	1.09	0.91	0.84	1.06	1.01	1.13	0.12

Table 3. continued

sample depth	3315	3420	3444	3473	3508	3611	3658	3724	3743	3781	3826	3847	3945
Instrumental Neutron Activation Analysis (INAA) in parts per million													
Cs	<0.2	<0.2	<0.2	0.3	0.5	<0.2	0.5	<0.2	<0.2	<0.2	0.2	<0.2	<0.2
Ba	833	39	95	97	312	165	258	200	61	127	424	60	194
Th	1.2	0.7	0.8	0.8	0.8	0.7	0.8	0.9	1.1	1.1	0.9	0.9	1.3
U	0.2	<0.1	0.3	<0.1	0.4	0.2	0.3	0.3	0.2	<0.1	<0.1	0.3	0.4
Ta	0.7	0.6	<0.3	0.6	0.6	<0.3	0.5	0.4	0.5	0.6	0.3	0.4	0.9
Sr	144	333	164	137	223	134	79	157	219	189	192	255	223
Hf	3.8	2.3	2.4	2.4	2.6	2.4	2.6	2.6	2.8	2.9	2.7	2.8	3.0
As	<1	1	<1	<1	<1	1	2	7	2	1	1	1	<1
Rare earth elements (in parts per million)													
La	24.0	8.0	8.8	8.7	9.2	8.7	8.9	9.4	10.8	10.6	10.1	10.4	11.3
Ce	51	20	22	22	23	22	23	24	26	27	24	25	27
Nd	26	11	13	14	15	13	14	15	16	16	14	15	18
Sm	5.58	3.03	3.44	3.37	3.55	3.34	3.35	3.46	3.78	3.87	3.54	3.67	3.89
Eu	1.95	1.06	1.14	1.18	1.20	1.15	1.12	1.23	1.26	1.30	1.22	1.24	1.30
Tb	0.9	0.6	0.6	0.6	0.7	0.7	0.6	0.7	0.8	0.7	0.7	0.7	0.8
Yb	3.43	2.04	2.32	2.33	2.32	2.20	2.32	2.32	2.43	2.43	2.32	2.43	2.58
Lu	0.53	0.31	0.33	0.36	0.34	0.34	0.34	0.36	0.37	0.39	0.36	0.38	0.41
CIPW (in weight percent)													
%AN	49.60	57.78	44.83	44.20	62.40	42.41	37.32		48.98	48.28	56.82	48.11	52.14
Q										0.65			
Or	11.97	0.74	2.42	2.42	0.28	3.49	4.12	13.49	1.12	1.18	7.40	0.68	3.47
Ab	23.92	23.91	35.25	32.43	22.91	36.11	30.48	10.69	30.42	30.29	22.78	30.58	27.87
An	23.54	32.72	28.65	25.69	38.02	26.59	18.15		29.20	28.27	29.97	28.36	30.36
Ne	0.14				1.08			32.82					
C			0.38	2.73		1.83	5.38						
Di	9.70	25.23			1.06			30.33	12.95	11.30	12.47	17.15	11.88
Hy		7.67	1.54	1.49		2.30	17.90		10.71	19.42	9.82	8.02	9.17
Wo													
Ol	16.56	1.48	22.70	26.82	26.97	20.66	15.39	1.69	6.66		8.17	6.07	7.57
Ac								7.85					
Mt	8.61	5.30	5.95	5.28	6.29	5.97	5.60	0.19	5.64	5.68	5.88	5.91	6.20
Il	4.33	2.51	2.72	2.76	2.98	2.65	2.63	2.66	2.83	2.80	2.97	2.82	3.07
Hem													
It													
Ap	1.23	0.44	0.39	0.40	0.42	0.40	0.37	0.36	0.47	0.41	0.53	0.41	0.41

REFERENCES CITED

Basaltic Volcanism Study Project, 1981, Pre-Tertiary continental flood basalts, *in* Basaltic volcanism on the terrestrial planets: New York, Pergamon Press, p. 60-67.

Brannon, J.C., 1984, Geochemistry of successive lava flows of the Keweenawan North Shore Volcanic Group: St. Louis, Mo., Washington University, Ph.D. dissertation, 312 p.

Cannon, W.F., and nine others, 2001, New map reveals original geology of North American Mid-continent rift: Eos, v. 82, no. 8, p. 97, 100-101.

Cullers, R.L., and Berendsen, P., 1993, Composition of rift-related igneous and sedimentary rocks of the Keweenawan Supergroup in the Poersch no. 1, 0Z-1, Finn, and Friederich wells, northeastern Kansas, *in* Braverman, M.S., ed., Current research on Kansas geology, summer, 1993: Kansas Geological Survey Bulletin 235, p. 57-72.

Davis, D.W., and Paces, J.B., 1990, Time resolution of geologic events on the Keweenaw Peninsula and implications for development of the Midcontinent rift system: Earth and Planetary Science Letters, v. 97, p. 54-64.

Davis, D.W., and Sutcliffe, R.H., 1985, U-Pb ages from the Nipigon plate and northern Lake Superior: Geological Society of America Bulletin, v. 96, p. 1572-1579.

Ewart, Anthony, 1979, A review of the mineralogy and chemistry of Tertiary-Recent dacitic, latitic, rhyolitic and related salic volcanic rocks, *in* Barker, Fred, ed., Trondhjemites, dacites and related rocks: New York, Elsevier Scientific Publications, p. 13-121.

Hughes, C.J., 1973, Spilites, keratophyres, and the igneous spectrum: Geological Magazine, v. 109, p. 513-527.

Irvine, T.N., and Baragar, W.R.A., 1971, A guide to the chemical classification of the common volcanic rocks: Canadian Journal of Earth Sciences, v. 8, p. 527-548.

Jensen, L.S., 1976, A new cation plot for classifying subalkalic volcanic rocks: Ontario Division of Mines, Ministry of Natural Resources, Miscellaneous Paper 66, 22 p.

LeBas, M.J., LeMaitre, R.W., Streckeisen, A.L., and Zanettin, Bruno, 1986, A chemical classification of volcanic rocks based on the total alkali-silica diagram: Journal of Petrology, v. 27, p. 745-750.

LeMaitre, R.W., 1984, A proposal by the IUGS subcommission on the systematics of igneous rocks for a chemical classification of volcanic rocks based on the total alkali-silica (TAS) diagram: Australian Journal of Earth Sciences, v. 31, p. 243-255.

Morey, G.B., 1977, Revised Keweenawan subsurface stratigraphy, southeastern Minnesota: Minnesota Geological Survey Report of Investigations 16, 67 p.

Morey, G.B., and Mudrey, M.G., Jr., 1972, Keweenawan volcanic rocks in east-central Minnesota, *in* Sims, P.K., and Morey, G.B., eds., Geology of Minnesota: A centennial volume: Minnesota Geological Survey, p. 425-435.

Mossler, J.H., and Tipping, R.G., 2000, Digital bedrock geologic map and bedrock topography of the Twin Cities Seven County Metropolitan area, Minnesota: Minnesota Geological Survey Miscellaneous Map Series M-104, scale 1:100,000.

Naiman, Z., Wirth, K.R., Miller, J.D., and Morey, G.B., 1996, Metamorphism of Chengwatana Volcanic Group near Taylors Falls and from Osseo core, Minnesota [abs.]: Institute on Lake Superior Geology, Proceedings, 42nd Annual Meeting, Cable, Wis., v. 42, pt. 1, p. 40-41.

Nicholson, S.W., 1992, Geochemistry, petrology, and volcanology of rhyolites of the Portage Lake Volcanics, Keweenaw Peninsula, Michigan: U.S. Geological Survey Bulletin 1970-B, 57 p.

Paces, J.B., 1988, Magmatic processes, evolution and mantle source characteristics contributing to the petrogenesis of Midcontinent rift basalts: Portage Lake basalts, Keweenaw Peninsula, Michigan: Houghton, Mich., Michigan Technological University, Ph.D. dissertation, 413 p.

Paces, J.B., and Davis, D.W., 1988, Duration of Midcontinent rift volcanism with estimates of subsidence rates, repose periods and magma production rates [abs.]: Eos, v. 69, p. 1479.

Palacas, J.G., Schmoker, J.W., Daws, T.A., Pawlewicz, M.J., and Anderson, R.R., 1990, Petroleum source-rock assessment of Middle Proterozoic (Keweenawan) sedimentary rocks, Eischeid #1 well, Carroll County, Iowa, *in* Anderson, R.R., ed., The Amoco M.G. Eischeid #1 deep petroleum test, Carroll County, Iowa: Iowa Department of Natural Resources, Geological Survey Bureau, Special Report Series 2, p. 119-134.

Palmer, H.C., and Davis, D.W., 1987, Paleomagnetism and U-Pb geochronology of Michipicoten Island: Precise calibration of the Keweenawan polar wander track: Precambrian Research, v. 37, p. 157-171.

Pearce, J.A., 1996, A user's guide to basalt discrimination diagrams, *in* Wyman, D.A., ed., Trace element geochemistry of volcanic rocks: Applications for massive sulfide exploration: Geological Association of Canada, Short Course Notes, v. 12, p. 79-113.

Pearce, J.A., and Cann, J.R., 1973, Tectonic setting of basic volcanic rocks determined using trace element analyses: Earth and Planetary Science letters, v. 19, p. 290-300.

Sims, P.K., and Zietz, I., 1967, Aeromagnetic and inferred Precambrian paleogeologic map of east-central Minnesota and part of Wisconsin: U.S. Geological Survey Map GP-563, scale 1:250,000.

Sun, S.S., and McDonough, W.F., 1989, Chemical and isotopic systematics of oceanic basalts: Implications for mantle composition and processes, *in* Saunders, A.D., and Norry, M.J., eds., Magmas in the ocean basins: Geological Society (London), Special Publication 42, p. 313-345.

Taylor, S.R., and McLennan, S.M., 1985, The continental crust: Its composition and evolution: Oxford, Blackwell Scientific, 328 p.

VanSchmus, W.R., and Hinze, W.J., 1985, The Midcontinent rift system: Annual Review of Earth and Planetary Sciences, v. 15, p. 345-383.

VanSchmus, W.R., Martin, M.W., Sprowl, D.R., Geissman, D.R., and Berendsen, P., 1990, Age, Nd and Pb isotopic composition, and magnetic polarity for subsurface samples of the 1,100 Ma Midcontinent rift: Geological Society of America, Abstracts with Program, v. 22, pt. A, p. 174.

Wilson, M., 1989, Igneous petrogenesis: London, Chapman and Hall, 466 p.

Wirth, K.R., Naiman, Z., Vervoort, J.D., Miller, J.D., and Morey, G.B., 1996, Geochemistry of Chengwatana Volcanic Group near Taylors Falls and from Osseo core, Minnesota [abs.]: Institute on Lake Superior Geology, Proceedings, 42nd Annual Meeting, Cable, Wis., v. 42, pt. 1, p. 66-67.

Zartman, R.E., Nicholson, S.W., Cannon, W.F., and Morey, G.B., 1997, U-Th-Pb zircon ages of some Keweenawan Supergroup rocks from the south shore of Lake Superior: Canadian Journal of Earth Sciences, v. 34, p. 549-561.

IC47